

# A perturbative renormalization group approach to light-front Hamiltonian

Takanori Sugihara \*

*Department of Physics, Kyushu University, Fukuoka 812-81, Japan*

Masanobu Yahiro †

*National University of Fisheries, Shimonoseki 759-65, Japan*

(November 15, 2017)

## Abstract

A perturbative renormalization group (RG) scheme for light-front Hamiltonian is formulated on the basis of the Bloch-Horowitz effective Hamiltonian, and applied to the simplest  $\phi^4$  model with spontaneous breaking of the  $Z_2$  symmetry. RG equations are derived at one-loop order for both symmetric and broken phases. The equations are consistent with those calculated in the covariant perturbation theory. For the symmetric phase, an initial cutoff Hamiltonian in the RG procedure is made by excluding the zero mode from the canonical Hamiltonian with an appropriate regularization. An initial cutoff Hamiltonian for the broken phase is constructed by shifting  $\phi$  as  $\phi \rightarrow \phi - v$  in the initial Hamiltonian for the symmetric phase. The shifted value  $v$  is determined on a renormalization trajectory. The minimum of the effective potential occurs on the trajectory.

---

\*e-mail : sugi1scp@mbox.nc.kyushu-u.ac.jp

†e-mail : yahiro@fish-u.ac.jp

## I. INTRODUCTION AND SUMMARY

Relativistic bound and scattering states of strongly interacting particles are not understood well. Quantum chromodynamics (QCD) is the typical case. Such a problem is solved by constructing a nonperturbative approach to relativistic quantum field theory. Light-Front Tamm-Dancoff theory (LFTD) [1] is a hopeful candidate for the approach. In LFTD, invariant masses of bound states are obtained by diagonalizing a light-front Hamiltonian after truncating the light-front Fock space. The truncation is what is called the Tamm-Dancoff approximation [2]. LFTD is precisely the Tamm-Dancoff approximation applied to light-front field theory. The approximation is believed to be reliable at least for low-energy states. This is really true in two-dimensional gauge theories [3,4], since the physical vacuum is trivial in the light-front field theory [5,6] and as the natural result the states may have simple structures.

The light-front field theory raises complicated renormalization issues, when it is applied to realistic four-dimensional field theories like QCD. The light-front counterterms have complex structure and even nonlocal in longitudinal direction, since infrared divergences in longitudinal momentum and ultraviolet divergences in transverse momentum arise simultaneously. The structure is investigated for QED with perturbation [7,8] and for the Yukawa model [9] with an approximate but nonperturbative manner.

As a powerful method for solving such complicated renormalization issues in light-front field theory, we consider Wilson's renormalization group (RG) [10], in which renormalization is achieved automatically by finding a fixed point and a renormalization trajectory ( a flow running out of the point ). Perry [11] applies the Minkowski-space version [12] of Wilson's RG for light-front Hamiltonian. Glazek and Wilson [13] formulate a new perturbative RG scheme for Hamiltonian by using a specially designed similarity transformation. The two RG schemes are based on perturbation and reliable for analyzes of RG flows near a Gaussian fixed point.

The basic RG procedure for Hamiltonian is the following:

- (1) A bare Hamiltonian is regularized by truncating the Fock space at a large cutoff energy  $\Lambda_0$ . The regularized Hamiltonian  $H_{\Lambda_0}$  is regarded as the initial Hamiltonian in the RG procedure.
- (2) The truncated space is separated into the lower- and higher-energy sectors. An effective Hamiltonian  $H_\Lambda$  for the lower-energy sector is constructed in a manner that it preserves physics of the lower-energy sector, while the higher-energy sector is eliminated. The cutoff is thus lowered to  $\Lambda$ . In the actual derivation of  $H_\Lambda$ , the finite transformation ( $\Lambda_0 \rightarrow \Lambda$ ) is expressed with successive small transformations ( $\Lambda_0 \rightarrow \Lambda_1 \rightarrow \dots \rightarrow \Lambda$ ), and the  $n$ -th effective Hamiltonian  $H_{\Lambda_n}$  is derived with perturbation from the  $(n-1)$ -th one  $H_{\Lambda_{n-1}}$ .
- (3) The cutoff  $\Lambda$  is rescaled to  $\Lambda_0$  by changing the energy scale, and field variables are also rescaled so that a fixed point may exist. In consequence,  $H_\Lambda$  is transformed into a new Hamiltonian  $H'_{\Lambda_0}$  with the initial cutoff  $\Lambda_0$ . The second and third steps progress from ultraviolet to infrared.

The main purpose of this paper is to propose a perturbative RG scheme which is more practical than those of Perry and of Głazek and Wilson. Our RG scheme differs from the two schemes in the second step. Perry uses the Bloch effective Hamiltonian [14] which contains an operator  $R$  obeying a nonlinear equation  $RP H_{\Lambda_0} \mathcal{P} - Q H_{\Lambda_0} Q R + RP H_{\Lambda_0} Q R - Q H_{\Lambda_0} \mathcal{P} = 0$ , where  $\mathcal{P}$  ( $\mathcal{Q}$ ) is a projector onto the lower- (higher-) energy sector. It is very hard to solve such a nonlinear equation without perturbation. Even if the equation is solved perturbatively by assuming that all matrix elements of  $R$  are small, the solution has infinitely large matrix elements, since the matrix elements contain vanishing energy differences in denominators. Thus, perturbation does not work for the Bloch effective Hamiltonian. The RG scheme of Głazek and Wilson also contains a nonlinear equation, but the “vanishing energy denominator” problem does not appear, since it is designed so that energy differences in denominators can be replaced by energy sums. As it has not been applied to realistic field theories so far, its application is highly expected. We then use the Bloch-Horowitz

[15] effective Hamiltonian instead of the Bloch one. This facilitates a perturbative RG procedure. This RG scheme is applied to the simplest  $\phi^4$  model with spontaneous breaking of the discrete symmetry  $\phi \rightarrow -\phi$ . Our results are summarized as follows.

(i) Our RG scheme based on the Bloch-Horowitz effective Hamiltonian is quite practical.

The scheme is free from the “vanishing energy denominator” problem, so that RG equations are easily derived with perturbation. The resultant RG flows depend on eigenenergies  $E_i$  of  $H_{\Lambda_0}$ , since so does the effective Hamiltonian. The dependence is negligible for  $\Lambda$  much larger than  $E_i$ . The state dependence becomes significant as  $\Lambda$  decreases, but it does not make any trouble. Renormalization is achieved by finding a renormalization trajectory for the lowest state with  $E_1$ . Renormalization trajectories for higher energy states are obtainable with LFTD from that for the lowest state. The renormalization trajectories, each with different  $E_i$ , converge on a fixed point as  $\Lambda$  goes to infinity. In principle, this RG scheme is applicable not only for light-front Hamiltonians but also for equal-time Hamiltonians.

(ii) Renormalization group (RG) equations for mass  $\mu$  and coupling  $\lambda$  are derived at one-loop order, where all irrelevant operators generated by RG transformation are removed as a reasonable approximation. The invariant mass regularization [11] is adopted in this paper, but it breaks covariance and cluster property, so the running mass and coupling constant depend on momenta of spectators if they exist. The dependence is, however, very weak, as long as  $\Lambda$  is at least several times larger than  $\mu$  and  $M_i$  which are assumed to be of order the physical mass scale  $\Lambda_{phys}$ . So it is neglected as a reasonable approximation in this paper. The regularization also excludes the zero mode (a mode with zero longitudinal momentum) from the canonical Hamiltonian. The zero mode is responsible for spontaneous symmetry breaking, that is, the order parameter  $\langle 0|\phi|0\rangle$  for the  $Z_2$  symmetry never becomes nonzero without the mode. This means that the RG equations calculated with the initial cutoff Hamiltonian are correct only for the symmetric phase. In fact, a flow diagram drawn with the RG equations

shows not only that two phases exist, but also that tachyons come out in the broken phase.

- (iii) In light-front field theory, Hamiltonians are different between the two phases, while their vacua are always trivial. Result (ii) indicates that for the symmetric phase the initial Hamiltonian  $H_{\Lambda_0}$  is obtained just by removing the zero mode from the canonical Hamiltonian with an appropriate regularization. A problem is how to construct another  $H_{\Lambda_0}$  valid for the broken phase. Once the zero mode is switched off, the system has to sit in the bottom of the effective potential. We then have to shift  $\phi$  as  $\phi \rightarrow \phi - v$  in the initial Hamiltonian for the symmetric phase. Once a renormalization trajectory is found,  $v$  is determined as a function of  $\Lambda$  on the trajectory.
- (iv) The RG equations for  $\mu$ ,  $\lambda$  and  $v$  calculated in the present framework are compared with those in the covariant perturbation theory. For  $\Lambda \gg \Lambda_{phys}$ , both agree with each other, except for the following point. In the covariant theory a contribution of the tadpole (Fig. 1) is explicitly calculated and then present in the RG equations. On the other hand, the contribution is removed in our normal ordered  $H_{\Lambda_0}$ , so it does not appear in our RG equations explicitly.
- (v) At the one-loop level, we find by using the present RG equations that  $\mu(\Lambda)^2 + \lambda(\Lambda)v(\Lambda)^2/6$  is invariant for any  $\Lambda$  and by calculating the effective potential that the RG invariant quantity is zero when the system sits in the bottom of the potential. The resultant relation  $\mu(\Lambda)^2 + \lambda(\Lambda)v(\Lambda)^2/6 = 0$  are thus a condition for the system to be in the bottom, and the renormalization trajectory should satisfy the relation. This is confirmed. A way of finding the relation without calculating the effective potential is furthermore presented.

Throughout all the results, we conclude that the present perturbative RG scheme is quite practical and valid at least near a Gaussian fixed point. This method is applicable for both the symmetric and broken phases. Application of the present method to QCD may not be

straightforward, since it is known in the equal-time field theory that the QCD vacuum is much more complicated than that of the present model. Further study on how to construct  $H_{\Lambda_0}$  in the QCD case is highly expected.

Section II presents our RG scheme and shows result (i). In section III, the scheme is applied to  $\phi^4$  model in 3+1 dimensions with spontaneous breaking of the  $Z_2$  symmetry. In subsections III A and III B, we derive RG equations for the symmetric phase to show result (ii). Subsection III C considers how to derive RG equations for the broken phase and shows result (iii) and a part of result (v). In subsection III D, we compare the RG equations with those calculated in the covariant perturbation theory and show results (iv) and (v). In Appendix A we evaluate loop integrals present in RG equations and show a part of result (ii).

## II. RENORMALIZATION GROUP SCHEME

A RG scheme is proposed along three steps (1)-(3) mentioned in section I. The scalar field theory is considered as an example.

As step (1), the light-front bare Hamiltonian is regularized with a boost-invariant regularization. As a feature, the bare Hamiltonian has no coupling between center-of-mass and intrinsic motions, indicating that the two types of motions are independent of each other. The regularization keeps the property. Among some possible boost-invariant regularizations, we take the invariant mass regularization [11], since some loop integrals appearing in the RG equations are analytically calculable.

In light-front kinematics a free particle with longitudinal and transverse momenta,  $\mathbf{k} \equiv (k^+, \mathbf{k}_\perp)$ , has an energy  $\epsilon_{\mathbf{k}} \equiv (\mathbf{k}_\perp^2 + \mu^2)/(2k^+)$ . An invariant mass  $M$  of an  $n$ -body Fock state, each particle with a momentum  $\mathbf{k}_i$ , is then defined as  $E = (\mathbf{P}_\perp^2 + M^2)/(2P^+)$  for the total energy  $E = \sum_{i=1}^n \epsilon_{\mathbf{k}_i}$  and the total momentum  $\mathbf{P} \equiv (P^+, \mathbf{P}_\perp) = \sum_{i=1}^n \mathbf{k}_i$ . The invariant mass regularization excludes all Fock states with  $M$  larger than an initial cutoff  $\Lambda_0$ . Since  $M$  diverges when  $k^+ = 0$ , the mode with  $k^+ = 0$  is removed here. The initial

cutoff Hamiltonian is denoted by  $H_{\Lambda_0}$ .

As step (2), the truncated Fock space is cut at  $M = \Lambda$  smaller than  $\Lambda_0$  by a finite amount, and separated into the lower and higher  $M$  sectors, i.e. the  $\mathcal{P}$  and  $\mathcal{Q}$  sectors. We use the Bloch-Horowitz effective Hamiltonian

$$H_{\Lambda}(M_i) = \mathcal{P}H_{\Lambda_0}\mathcal{P} + \mathcal{P}V\mathcal{Q}\frac{1}{E_i - \mathcal{Q}H_{\Lambda_0}\mathcal{Q}}\mathcal{Q}V\mathcal{P}, \quad (2.1)$$

where  $H_{\Lambda_0}$  is composed of the free and interaction parts,  $H_0$  and  $V$ . The effective Hamiltonian has been derived with the projectors  $\mathcal{P}$  and  $\mathcal{Q}$  from the Schrödinger equation  $H_{\Lambda_0}|\Psi_i\rangle = E_i|\Psi_i\rangle$ , where the  $i$ -th eigenmass  $M_i$  is determined from  $E_i$  with the dispersion relation  $E_i = (\mathbf{P}_{\perp}^2 + M_i^2)/(2P^+)$ . Eigenvalues and eigenstates,  $E'_i$  and  $|\Psi'_i\rangle$ , of  $H_{\Lambda}$  satisfy  $E'_i = E_i$  and  $|\Psi'_i\rangle = \mathcal{P}|\Psi_i\rangle$ . The effective Hamiltonian thus preserves physics of the  $\mathcal{P}$  sector.

In principle, the finite transformed Hamiltonian  $H_{\Lambda}$  is derivable with (2.1) from  $H_{\Lambda_0}$ . In practice, however, the finite transformation ( $\Lambda_0 \rightarrow \Lambda$ ) is described with successive small transformations ( $\Lambda_0 \rightarrow \Lambda_1 \rightarrow \dots \rightarrow \Lambda$ ), and the  $n$ -th Hamiltonian  $H_{\Lambda_n}$  is derived from the  $(n-1)$ -th one with the Bloch-Horowitz effective Hamiltonian formalism. This prescription has a merit; see subsection III B. The  $n$ -th effective Hamiltonian  $H_{\Lambda_n}$  includes the  $\mathcal{Q}$ -space Green function  $G \equiv 1/(E_i - \mathcal{Q}H_{\Lambda_{n-1}}\mathcal{Q})$ , where the  $\mathcal{Q}$  space is  $\Lambda_n < M \leq \Lambda_{n-1}$  and the  $\mathcal{P}$  space is  $M \leq \Lambda_n$ . The Green function is related to the free one  $G_0 \equiv 1/(E_i - \mathcal{Q}H_0\mathcal{Q})$  as

$$G = G_0 + G_0\mathcal{Q}V\mathcal{Q}G, \quad (2.2)$$

where use has been made of the identity  $A^{-1} - B^{-1} = B^{-1}(B - A)A^{-1}$ . The full Green function  $G$  is obtained by solving (2.2) perturbatively. When  $E_i$  is above the two-body threshold energy  $E_{thresh} = \epsilon_{\mathbf{k}_1} + \epsilon_{\mathbf{k}_2}$ , we must solve a scattering problem by replacing  $E_i$  by  $E_i + i\delta$ .

The RG procedure is completed by the scale transformation of Step (3). The effective Hamiltonian  $H_{\Lambda}$  is transformed into a new Hamiltonian  $H'_{\Lambda_0}$  with a cutoff  $\Lambda_0$  by scaling transverse momenta  $\mathbf{k}_{\perp}$  as

$$\mathbf{k}_\perp = \frac{\Lambda}{\Lambda_0} \mathbf{k}'_\perp, \quad (2.3)$$

since the  $\mathcal{P}$  space ( $M < \Lambda$ ) is expanded to the  $\mathcal{P} + \mathcal{Q}$  space ( $M < \Lambda_0$ ) by the transformation; precisely speaking, a total energy of an  $n$ -body Fock state belonging to the  $\mathcal{P}$  space is varied in the region

$$0 < \sum_{i=1}^n \frac{\mu^2 + \mathbf{k}_{\perp i}^2}{2k_i^+} < \frac{\Lambda^2 + \mathbf{P}_\perp^2}{2P^+}, \quad (2.4)$$

and the scaling expands the region to

$$0 < \sum_{i=1}^n \frac{(\Lambda_0/\Lambda)^2 \mu^2 + \mathbf{k}'_{\perp i}{}^2}{2k_i^+} < \frac{\Lambda_0^2 + \mathbf{P}'_\perp{}^2}{2P^+}. \quad (2.5)$$

In addition to the transverse momenta, the field variables  $\phi(\mathbf{k})$  ( the creation and annihilation operators,  $a^\dagger(\mathbf{k})$  and  $a(\mathbf{k})$  ) and the Hamiltonian  $H_\Lambda$  are also scaled to [11]

$$\begin{aligned} \phi(k^+, \mathbf{k}_\perp) &= \zeta \phi'(k^+, \mathbf{k}'_\perp), \\ H_\Lambda(\phi(k^+, \mathbf{k}_\perp)) &= \eta^{-1} H'_{\Lambda_0}(\phi'(k^+, \mathbf{k}'_\perp)). \end{aligned} \quad (2.6)$$

The constants  $\zeta$  and  $\eta$  are determined so that fixed points can exist. There exists a Gaussian fixed point in four dimensional  $\phi^4$  model. At the fixed point,  $H_{\Lambda_0}$  is reduced to the free part  $H_0(\Lambda_0; \phi(k^+, \mathbf{k}_\perp))$ , so the Bloch-Horowitz effective Hamiltonian  $H_\Lambda$  and the rescaled one  $H'_{\Lambda_0}$  are easily derived as  $H_\Lambda = \mathcal{P}H_0(\Lambda_0; \phi(k^+, \mathbf{k}_\perp))\mathcal{P}$  and  $H'_{\Lambda_0} = \eta H_0(\Lambda_0; \zeta \phi'(k^+, \mathbf{k}'_\perp))$ . The constants  $\zeta$  and  $\eta$  are determined from the condition that  $H'_{\Lambda_0} = H_{\Lambda_0}$ . The constants thus obtained are [11]

$$\zeta = (\Lambda/\Lambda_0)^{-1}, \quad \eta = (\Lambda/\Lambda_0)^{-2}. \quad (2.7)$$

Adopting the Bloch-Horowitz effective Hamiltonian in step (2) makes the present RG procedure practical, because we can easily solve Eq.(2.2) with perturbation. For  $E_i < E_{thresh}$ , the solution contain energy differences  $E_i - E$  in denominators, where  $E = (\mathbf{P}_\perp^2 + M^2)/(2P^+)$  and  $M$  belongs to the  $\mathcal{Q}$  space. The denominators never vanish, because  $E \geq E_{thresh}$  for any  $\Lambda$  and there exists an energy gap between  $E_i$  and  $E_{thresh}$ . The present RG scheme is thus free from the “vanishing energy denominator” problem.

The effective Hamiltonian is not Hermitian, since it depends on  $M_i$ . However, it does not make any trouble. An only difference from the ordinary RG is that the running mass  $\mu$  and the running coupling  $\lambda$  depend on not only  $\Lambda$  but also  $M_i$ . The  $M_i$  dependence or the state dependence becomes negligible for  $\Lambda \gg M_i$ , since on the right hand side of (2.2)  $E_i - E = (M_i - M)/(2P^+) \approx -M/(2P^+)$  as a result of  $M_i \ll \Lambda < M < \Lambda_0$ . We are interested in low-energy physics, so  $M_i$  is considered to be of order  $\Lambda_{phys}$ . The parameters  $\mu$  and  $\lambda$  thus has no  $M_i$  dependence for  $\Lambda \gg \Lambda_{phys}$ .

When  $\Lambda$  is of order  $\Lambda_{phys}$ , the  $M_i$  dependences of  $\mu$  and  $\lambda$  become significant. For any scattering state ( with  $E_i > E_{thresh}$  ),  $M_i$  is just an input parameter determined from the initial condition of scattering, so one can draw a RG flow. For bound states ( with  $E_i < E_{thresh}$  ), on the contrary,  $M_i$ 's are unknown. Only an exception is the lowest mass  $M_1$ , since it is set to the physical mass  $M_{phys}$  as a renormalization condition. Other  $M_i$ 's each are determined in a prescription mentioned below.

Our renormalization procedure starts with drawing a flow diagram for the lowest state by solving RG equations under the condition  $M_1 = M_{phys}$ . It essentially ends up with finding out a renormalization trajectory in the flow diagram, since renormalization trajectories for excited states are obtainable from that for the lowest state just by replacing  $M_1$  by  $M_i$ , if  $M_i$  is given; this is obvious, if one knows analytic solution to RG equations. All the trajectories converge at a fixed point as  $\Lambda$  goes to infinity. The  $M_i$ 's are given for scattering states, but not for bound states. The invariant masses of bound states are obtained as follows. Suppose that the trajectory for the lowest state is found. We choice a point A on the trajectory at which  $\Lambda$  is much larger than  $\Lambda_{phys}$ ; the cutoff is denoted by  $\Lambda_A$ . If one can solve the Schrödinger equation  $\{H_{\Lambda_A}(M_1) - (\mathbf{P}_\perp^2 + M_i'^2)/(2P^+)\}|\Psi_i'\rangle = 0$  with LFTD, the approximate eigenvalues  $M_i'^2$  each contain errors of order  $(M_i'^2 - M_1^2)/\Lambda_A^2$ . The errors are thus negligible for low-lying states. For such large Fock space, LFTD may not be so practical, since it demands a large number of basis functions to diagonalize the Hamiltonian accurately. If one comes across this problem in practical calculations, take the following self-consistent way as a second choice. First draws a RG flow starting from point A with

an initial estimate  $M_i^{(1)}$  of  $M'_i$ . Next choose a point B on the flow at which  $\Lambda$  is of order  $\Lambda_{phys}$ . For such small  $\Lambda$  LFTD is a powerful tool, unless  $\lambda$  is very large. At point B one can then diagonalize the effective Hamiltonian to get the second estimate  $M_i^{(2)}$ . Again, draw a flow running out of point A with  $M_i^{(2)}$ , and so on. This procedure progresses until we get  $M_i^{(n+1)} = M_i^{(n)}$ . The mass thus obtained is equal to the approximate mass  $M'_i$ .

### III. $\phi^4$ MODEL

#### A. The first step of RG procedure

Our convention for light-front coordinates is  $x^\pm = (x_0 \pm x_3)/\sqrt{2}$  and  $x_\perp^i \equiv x^i (i = 1, 2)$ . The quantity  $x^+$  is chosen as the "time" direction along which all the states are evolved, so  $x^-$  and  $x_\perp$  become the longitudinal and transverse directions. The metric tensor is then given by  $g^{+-} = g^{-+} = g_{+-} = g_{-+} = 1, g^{ii} = g_{ii} = -1 (i = 1, 2)$  and zero for others.

The Lagrangian density of  $\phi^4$  model in 4 dimensions is

$$\mathcal{L} = \frac{1}{2} \partial_\mu \phi \partial^\mu \phi - \frac{\mu^2}{2} \phi^2 - \frac{\lambda}{4!} \phi^4 \quad (3.1)$$

for a real scalar field  $\phi$ . The commutation relation for the field derived with the Schwinger's action principle [16] is

$$[\phi(x), \partial_- \phi(y)]_{x^+ = y^+} = \frac{i}{2} \delta^3(\mathbf{x} - \mathbf{y}). \quad (3.2)$$

The field is expanded in terms of free waves at  $x^+ = 0$ ,

$$\phi(\mathbf{x}) = \int \frac{d^3 \mathbf{k}}{\sqrt{(2\pi)^3 2k^+}} [a(\mathbf{k}) e^{-ik^+ x^- + i\mathbf{k}_\perp \cdot \mathbf{x}_\perp} + a^\dagger(\mathbf{k}) e^{ik^+ x^- - i\mathbf{k}_\perp \cdot \mathbf{x}_\perp}], \quad (3.3)$$

where

$$\int d^3 \mathbf{k} \equiv \int_0^{+\infty} dk^+ \int_{-\infty}^{+\infty} d\mathbf{k}_\perp. \quad (3.4)$$

Inserting this form into (3.2) yields a relation

$$[a(\mathbf{k}), a^\dagger(\mathbf{k}')] = \delta^3(\mathbf{k} - \mathbf{k}') \quad (3.5)$$

between the coefficients of expansion for positive  $k^+$  and  $k'^+$ . Obviously,  $a(\mathbf{k})$  and  $a^\dagger(\mathbf{k})$  with positive  $k^+$  are annihilation and creation operators for the Fock vacuum. As an important feature of light-front field theory, furthermore, they are annihilation and creation operators also for the true vacuum  $|0\rangle$ , since it is proven that  $a(\mathbf{k})|0\rangle = 0$  for positive  $k^+$  [5]. This indicates that the true vacuum is trivial in light-front field theory, at least as far as the zero mode is neglected; it is still true even after the zero mode is included explicitly with an appropriate way [6]. The Fock space is then constructed by acting the creation operator on the true vacuum:  $|\mathbf{k}_1, \mathbf{k}_2, \dots, \mathbf{k}_n\rangle \equiv \prod_{i=1}^n a^\dagger(\mathbf{k}_i)|0\rangle$ .

The Hamiltonian derived from the energy-momentum tensor [16] is

$$H = \int d^3x \left\{ \frac{1}{2} \left[ \sum_{i=1}^2 (\partial_i \phi)^2 + \mu^2 \phi^2 \right] + \frac{\lambda}{4!} : \phi^4 : \right\}, \quad (3.6)$$

where we have removed the tadpole (Fig. 1) by normal ordering the interaction term. The Hamiltonian is rewritten into

$$H_{\Lambda_0} = H_0 + V, \quad (3.7)$$

$$H_0 = \sum_{n=1} \frac{1}{n!} \int \left[ \prod_{i=1}^n d\mathbf{k}_i \right] \theta(\epsilon_{\Lambda_0} - \sum_{i=1}^n \epsilon_{\mathbf{k}_i}) \left[ \sum_{i=1}^n \epsilon_{\mathbf{k}_i} \right] \times |\mathbf{k}_1, \mathbf{k}_2, \dots, \mathbf{k}_i\rangle \langle \mathbf{k}_1, \mathbf{k}_2, \dots, \mathbf{k}_i|, \quad (3.8)$$

$$V = \sum_{n=2} v_{n,n} + \sum_{n=1} (v_{n+2,n} + v_{n,n+2}), \quad (3.9)$$

where

$$\begin{aligned} v_{n,n} &\equiv \frac{3\bar{\lambda}}{2(n-2)!} \int \left[ \frac{\prod_{i=1}^n d\mathbf{k}_i}{\sqrt{k_{n-1}^+ k_n^+}} \right] \left[ \frac{\prod_{i=1}^n d\mathbf{k}'_i}{\sqrt{k'_{n-1}^+ k_n'^+}} \right] \delta^3 \left( \sum_{i=1}^n \mathbf{k}_i - \sum_{i=1}^n \mathbf{k}'_i \right) \\ &\quad \times \prod_{i=1}^{n-2} \delta^3(\mathbf{k}_i - \mathbf{k}'_i) \theta(\epsilon_{\Lambda_0} - \sum_{i=1}^n \epsilon_{\mathbf{k}_i}) \theta(\epsilon_{\Lambda_0} - \sum_{i=1}^n \epsilon_{\mathbf{k}'_i}) \\ &\quad \times |\mathbf{k}_1, \dots, \mathbf{k}_n\rangle \langle \mathbf{k}'_1, \dots, \mathbf{k}'_n|, \\ v_{n,n+2} &= [v_{n+2,n}]^\dagger \\ &\equiv \frac{\bar{\lambda}}{(n-1)!} \int \left[ \frac{\prod_{i=1}^n d\mathbf{k}_i}{\sqrt{k_n^+}} \right] \left[ \frac{\prod_{i=1}^{n+2} d\mathbf{k}'_i}{\sqrt{k_n'^+ k_{n+1}'^+ k_{n+2}'^+}} \right] \delta^3 \left( \sum_{i=1}^n \mathbf{k}_i - \sum_{i=1}^{n+2} \mathbf{k}'_i \right) \\ &\quad \times \prod_{i=1}^{n-1} \delta^3(\mathbf{k}_i - \mathbf{k}'_i) \theta(\epsilon_{\Lambda_0} - \sum_{i=1}^n \epsilon_{\mathbf{k}_i}) \theta(\epsilon_{\Lambda_0} - \sum_{i=1}^{n+2} \epsilon_{\mathbf{k}'_i}) \\ &\quad \times |\mathbf{k}_1, \dots, \mathbf{k}_n\rangle \langle \mathbf{k}'_1, \dots, \mathbf{k}'_{n+2}|, \end{aligned} \quad (3.10)$$

where  $\bar{\lambda} = \lambda/4!(2\pi)^3$ ,  $\epsilon_{\mathbf{k}} \equiv (\mathbf{k}_{\perp}^2 + \mu^2)/(2k^+)$  and  $\epsilon_{\Lambda_0} \equiv (\mathbf{P}_{\perp}^2 + \Lambda_0^2)/(2P^+)$ . The total energy and momentum of an  $n$ -body state  $|\mathbf{k}_1, \mathbf{k}_2, \dots, \mathbf{k}_n\rangle$  satisfies the dispersion relation  $E = (\mathbf{P}_{\perp}^2 + M^2)/(2P^+)$ , so the invariant mass  $M$  of the state is represented by the Jacobi variables,  $x_i$  and  $\mathbf{r}_i$  ( $i = 1$  to  $n$ ), as

$$M^2 = \sum_{i=1}^n \frac{\mathbf{r}_{i\perp}^2 + \mu^2}{x_i^+} \geq (n\mu)^2, \quad (3.11)$$

where

$$\mathbf{k}_i \equiv (x_i P^+, x\mathbf{P}_{\perp} + \mathbf{r}_i). \quad (3.12)$$

One of the Jacobi variables is a dependent variable, since  $\sum_{i=1}^n x_i = 1$  and  $\sum_{i=1}^n \mathbf{r}_i = 0$  in consequence of  $\mathbf{P} = \sum_{i=1}^n \mathbf{k}_i$ . The  $x_i$  can vary from 0 to 1 and two components of the vector  $\mathbf{r}_i \equiv (r_i^1, r_i^2)$  from  $-\infty$  to  $\infty$ . The invariant mass  $M$  becomes minimum  $n\mu$  when  $\mathbf{r}_i = 0$  and  $x_i = 1/n$  for all  $i$ , and it diverges at  $r_i^j = \infty$  or at  $x_i = 0$ . The ultraviolet and infrared divergences are simultaneously excluded by the invariant-mass regularization  $M < \Lambda_0$ . The Hamiltonian (3.7) has already been regularized with this, that is, with the step functions  $\theta$  appearing in the momentum integrations. Here, it should be noted that the Hamiltonian does not include the zero mode at all. The Fock vacuum is obviously an eigenstate of the Hamiltonian, indicating that the physical vacuum is trivial. A center-of-mass motion is decoupled from internal motions in the Hamiltonian, since it does not contain any interaction between the two motions. This property is not broken by the invariant-mass regularization.

The light-cone quantization mentioned does not treat the zero mode properly [5,17]. As shown in subsection III B, it is needless for the symmetric phase, but not for the broken one. In principle the zero mode is treat-able by quantizing the theory in a spatial box  $-L < x^- \leq L$  under the periodic boundary condition, but in practice the procedure does not seem feasible, as mentioned in subsection III C. Ohio group suggests to add counterterms to the regularized Hamiltonian which does not contain the zero mode [11,18,19]. An aim of the present paper is to support the suggestion.

## B. The second and third steps of RG procedure

The second step of our RG procedure starts with dividing the finite transformation ( $\Lambda_0 \rightarrow \Lambda$ ) into successive small transformations ( $\Lambda_0 \rightarrow \Lambda_1 \rightarrow \dots \rightarrow \Lambda$ ). For the  $n$ -th small transformation,  $G$  is obtained by solving  $G = G_0 + G_0 \mathcal{Q}V \mathcal{Q}G$  perturbatively, where the projectors  $\mathcal{P}$  and  $\mathcal{Q}$  are defined as

$$\begin{aligned} \mathcal{P}|\mathbf{k}_1, \mathbf{k}_2, \dots, \mathbf{k}_n\rangle &\equiv \theta(\epsilon_{\Lambda_n} - \epsilon)|\mathbf{k}_1, \mathbf{k}_2, \dots, \mathbf{k}_n\rangle, \\ \mathcal{Q}|\mathbf{k}_1, \mathbf{k}_2, \dots, \mathbf{k}_n\rangle &\equiv \theta(\epsilon_{\Lambda_{n-1}} - \epsilon)\theta(\epsilon - \epsilon_{\Lambda_n})|\mathbf{k}_1, \mathbf{k}_2, \dots, \mathbf{k}_n\rangle, \end{aligned} \quad (3.13)$$

for any state having the total energy  $\epsilon$ . As shown in (3.11),  $\Lambda_n$  should be larger than  $\mu$ , so the one-body Fock state (with  $M = \mu$ ) can not be in the  $\mathcal{Q}$  space. Any diagram including the one-body state then does not contribute to the  $\mathcal{Q}$ -space Green function  $G$ .

In this paper we make one-loop approximation and neglect all irrelevant operators produced by the RG procedure as a reasonable approximation. A perturbative expansion of the Bloch-Horowitz Hamiltonian is then calculated up to second order in  $\lambda$ , that is,  $H_\Lambda(M_i) = \mathcal{P}H_0\mathcal{P} + \mathcal{P}V\mathcal{P} + \mathcal{P}V\mathcal{Q}G_0\mathcal{Q}V\mathcal{P} + O(V^3)$ . The second-order correction  $\mathcal{P}V\mathcal{Q}G_0\mathcal{Q}V\mathcal{P}$  generates two-, four- and six-point vertices, but the six-point one is neglected, because it is an irrelevant operator. The correction is obtained by calculating the matrix elements  $\langle \mathbf{k}_1, \mathbf{k}_2, \dots, \mathbf{k}_n | \mathcal{P}V\mathcal{Q}G_0\mathcal{Q}V\mathcal{P} | \mathbf{k}'_1, \mathbf{k}'_2, \dots, \mathbf{k}'_m \rangle$  separately.

Matrix elements of  $\mathcal{P}(V + V\mathcal{Q}G_0\mathcal{Q}V)\mathcal{P}$  between two-body Fock states are composed of four-point vertices displayed in Fig. 2. In our all diagrams, time flows toward the right. The longitudinal and transverse momenta are conserved at each vertex, and all particles are on shell. A net contribution of the diagrams becomes

$$\mathcal{P}(v_{22} + v_{22}G_0v_{22})\mathcal{P} = \bar{\lambda}(1 + 9\bar{\lambda}A)\mathcal{P}v_{22}\mathcal{P}. \quad (3.14)$$

The effective interaction has the same form as  $V$ , but with a new coupling constant  $\bar{\lambda}(\Lambda_n) = \bar{\lambda}(\Lambda_{n-1})\{1 + 9\bar{\lambda}(\Lambda_{n-1})A\}$ , where  $A$  is a loop integral defined as

$$A \equiv \frac{1}{2} \int \left[ \prod_{i=1}^4 \frac{d\mathbf{k}_i}{\sqrt{k_i^+}} \right] \delta^3(\mathbf{P} - \sum_{i=1}^2 \mathbf{k}_i) \langle \mathbf{k}_1, \mathbf{k}_2 | G_0 | \mathbf{k}_3, \mathbf{k}_4 \rangle$$

$$\begin{aligned}
&= \int \left[ \prod_{i=1}^2 \frac{d\mathbf{k}_i}{k_i^+} \right] \delta^3(\mathbf{P} - \sum_{i=1}^2 \mathbf{k}_i) F(\mathbf{k}_1, \mathbf{k}_2) \\
&= I_A(\Lambda_{n-1}, \mu(\Lambda_{n-1}), M_i) - I_A(\Lambda_n, \mu(\Lambda_{n-1}), M_i)
\end{aligned} \tag{3.15}$$

for

$$F(\mathbf{k}_1, \mathbf{k}_2, \dots, \mathbf{k}_n) \equiv \frac{\theta(\epsilon_{\Lambda_{n-1}} - \sum_{i=1}^n \epsilon_{\mathbf{k}_i}) \theta(\sum_{i=1}^n \epsilon_{\mathbf{k}_i} - \epsilon_{\Lambda})}{E_i - \sum_{i=1}^n \epsilon_{\mathbf{k}_i}}. \tag{3.16}$$

The loop integral  $A$  is obtained with an analytic function  $I_A$  defined in Appendix A. The function depends on the cutoff,  $\mu(\Lambda_{n-1})$  and  $M_i$ , but not on  $\mathbf{P}$ . Hereafter, it is assumed that  $\Lambda_0 \gg \Lambda_{phys}$  and  $M_i$  and  $\mu(\Lambda_{n-1})$  are of order  $\Lambda_{phys}$ . For  $\Lambda_n \gg \Lambda_{phys}$ ,  $A$  becomes  $4\pi t$ , where  $t = \ln |\Lambda_n / \Lambda_{n-1}|$ .

Matrix elements of  $\mathcal{P}(V + V\mathcal{Q}G_0\mathcal{Q}V)\mathcal{P}$  between three-body states are also calculated in a similar way. All diagrams contributing to the elements are also in Fig. 2, but with a spectator added. An example is shown in Fig. 3. The diagrams describe four-point vertices, since one of three particles is a spectator. A net contribution of these diagrams is

$$\begin{aligned}
&\mathcal{P}(v_{33} + v_{33}G_0v_{33})\mathcal{P} \\
&= \frac{3}{2} \int \left[ \prod_{i=1}^4 \frac{d\mathbf{k}_i}{\sqrt{k_i^+}} \right] d\mathbf{p} \delta^3(\sum_{i=1}^2 \mathbf{k}_i - \sum_{i=3}^4 \mathbf{k}_i) \theta(\epsilon_{\Lambda} - \sum_{i=1}^2 \epsilon_{\mathbf{k}_i}) \theta(\epsilon_{\Lambda} - \sum_{i=3}^4 \epsilon_{\mathbf{k}_i}) \\
&\quad \times \bar{\lambda}(1 + 9\bar{\lambda}B(\mathbf{p})) |\mathbf{k}_1, \mathbf{k}_2, \mathbf{p}\rangle \langle \mathbf{k}_3, \mathbf{k}_4, \mathbf{p}|,
\end{aligned} \tag{3.17}$$

where

$$B(\mathbf{p}) \equiv \int \left[ \prod_{i=1}^2 \frac{d\mathbf{k}'_i}{k_i^+} \right] \delta^3(\mathbf{P} - \sum_{i=1}^2 \mathbf{k}'_i - \mathbf{p}) F(\mathbf{k}'_1, \mathbf{k}'_2, \mathbf{p}). \tag{3.18}$$

The loop integral  $B(\mathbf{p})$  depends on  $\mathbf{p}$ , a momentum of the spectator. As shown in Fig. 4 and Appendix A,  $B(\mathbf{p})$  little differs from  $A$  for  $\Lambda_n \gg \Lambda_{phys}$ , but the difference becomes significant as  $\Lambda_n$  decreases; it is appreciable at  $\Lambda_n \sim 10\Lambda_{phys}$  and sizable at  $\Lambda_n \sim 5\Lambda_{phys}$ . This allows  $H_{\Lambda_n}$  to depend on the momentum of the spectator and the number of particles in the initial and final states. The dependences stem from the fact that the invariant mass regularization adopted breaks covariance and cluster decomposition. In this paper  $B(\mathbf{p})$  is set to  $A$  as a reasonable approximation, and  $\Lambda_n$  is then considered to be larger than  $10\Lambda_{phys}$ .

Only an exception is subsection III D in which the effective potential is calculated from a solution at the small  $\Lambda$  limit to RG equations. In this sense the calculation contains errors to some extent. A way of treating the spectator dependence explicitly is proposed in [11]. It may be useful for the present RG scheme, when one has to treat the dependence accurately.

Other matrix elements of  $\mathcal{P}(V + V\mathcal{Q}G_0\mathcal{Q}V)\mathcal{P}$  are also derivable in a similar fashion:

$$\begin{aligned}
\mathcal{P}(v_{31} + v_{33}G_0v_{31})\mathcal{P} &= [\mathcal{P}(v_{13} + v_{13}G_0v_{33})\mathcal{P}]^\dagger \\
&= \int \left[ \prod_{i=1}^4 \frac{d\mathbf{k}_i}{\sqrt{k_i^+}} \right] \theta(\epsilon_{\Lambda_1} - \sum_{i=1}^3 \epsilon_{\mathbf{k}_i}) \theta(\epsilon_{\Lambda_1} - \epsilon_{\mathbf{k}_4}) \delta^3(\sum_{i=1}^3 \mathbf{k}_i - \mathbf{k}_4) \\
&\quad \times \bar{\lambda}(\Lambda_{n-1}) \{1 + 9\bar{\lambda}(\Lambda_{n-1})B(\mathbf{k}_3)\} |\mathbf{k}_1, \mathbf{k}_2, \mathbf{k}_3\rangle \langle \mathbf{k}_4| \\
&\approx \bar{\lambda}(\Lambda_{n-1}) \{1 + 9\bar{\lambda}(\Lambda_{n-1})A\} \mathcal{P}v_{33}\mathcal{P}.
\end{aligned} \tag{3.19}$$

Figure 5 shows a unique one-loop diagram contributing to the matrix element  $\mathcal{P}(v_{31} + v_{33}G_0v_{31})\mathcal{P}$ . No one-loop diagram contributes to the matrix element  $\mathcal{P}v_{13}G_0v_{31}\mathcal{P}$ , indicating that the element vanishes within the present approximation.

The effective Hamiltonian  $H_{\Lambda_n}$  thus obtained holds the same form as  $H_{\Lambda_{n-1}}$ , but with new parameters

$$\bar{\lambda}(\Lambda_n) = \bar{\lambda}(\Lambda_{n-1}) \{1 + 9\bar{\lambda}(\Lambda_{n-1})A\}, \quad \mu(\Lambda)^2 = \mu(\Lambda_{n-1})^2. \tag{3.20}$$

Taking the limit  $\Lambda_n \rightarrow \Lambda_{n-1}$  leads to RG equations

$$\frac{d\lambda}{dt} = \frac{3\zeta}{4\pi} \frac{dI_A(\Lambda, \mu(\Lambda))}{dt} \lambda^2 + O(\hbar^2), \quad \frac{d\mu^2}{dt} = 0 + O(\hbar^2), \tag{3.21}$$

where  $\zeta = \hbar/(16\pi^2)$  and  $t = \ln(\Lambda/\Lambda_0)$ . For  $\Lambda \gg \Lambda_{phys}$ , the right hand side of the first equation tends to  $3\zeta\lambda^2$ . The equations are consistent with those calculated in the covariant perturbation theory, as shown in subsection III D. The right hand side originally included a partial derivative  $\partial I_A(\Lambda, \mu(\Lambda))/\partial t$  with  $\mu(\Lambda)$  fixed, but it has been replaced by  $dI_A/dt$ . The replacement is correct in this case, because of  $d\mu/dt = 0$ . Even if  $d\mu/dt \neq 0$  just as in the case of subsection III C, one can make the same replacement to derive RG equations at one-loop level, since  $dI_A/dt = \partial I_A/\partial t + O(\hbar)$  as a result of  $d\mu/dt = O(\hbar)$ . The solution to (3.21) is

$$\lambda(\Lambda) = \frac{\lambda_0}{1 - 3\zeta\tilde{A}\lambda_0/(4\pi)}, \quad \mu(\Lambda)^2 = \mu_0^2, \quad (3.22)$$

where  $\lambda_0 = \lambda(\Lambda_0)$ ,  $\mu_0 = \mu(\Lambda_0)$  and  $\tilde{A} = I_A(\Lambda_0, \mu(\Lambda_0)) - I_A(\Lambda, \mu(\Lambda))$ . Expanding the solution  $\lambda(\Lambda)$  in power of  $A$ , one can find that it contains not only contributions of the one-loop diagrams (Fig. 2) but also those of the ladder diagrams, although for each small transformation only the one-loop diagrams have been taken into account.

The RG procedure ends up with the scale transformation  $T$  of (2.4) and (2.6), where it is assumed that there exists only a Gaussian fixed point in the present model. The transformed Hamiltonian  $H'_{\Lambda_0} \equiv T[H_\Lambda]$  has parameters  $\lambda(\Lambda)' = \lambda(\Lambda)$  and  $\mu(\Lambda)'^2 = (\Lambda_0/\Lambda)^2\mu(\Lambda)^2$ . The running coupling  $\lambda(\Lambda)'$  depends not only on  $\Lambda$ , but also on the eigenvalue  $M_i$  of  $H_{\Lambda_0}$  through  $\tilde{A}$ . In the limit  $\Lambda = \infty$ , however, the coupling tends to  $\lambda_0/(1 - 3\zeta\lambda_0 t)$ , indicating no  $M_i$  dependence. The mass parameter  $\mu(\Lambda)$  present in  $H_\Lambda$  has no  $\Lambda$  dependence and then equal to the lowest mass  $M_1$ , so that the corresponding parameter  $\mu(\Lambda)'$  in the transformed Hamiltonian  $T[H_\Lambda]$  behaves as  $M_1\Lambda_0/\Lambda$ . We then draw a flow diagram for the lowest state by setting  $M_i = M_1 = M_{phys}$  in  $\tilde{A}$  as a renormalization condition. The diagram presented in Fig. 6 shows, as expected, that there exists a renormalization trajectory on the positive  $\mu'^2$  axis. On the axis  $\lambda'$  is always zero, indicating that the present model is trivial. Once the trajectory is found for the lowest state, renormalization trajectories for other states are obtainable from the one for the lowest state by replacing  $M_1$  by invariant masses of the excited states, if they are known. In the present case, such a state-dependence does not appear as a reflection of the triviality, that is, all the trajectories exist on the positive  $\mu'^2$  axis,

There appear two phases in Figure 6; a critical line between the two is on the positive  $\lambda'$  axis. A phase present in the first quadrant ( $\lambda' \geq 0$  and  $\mu'^2 \geq 0$ ) is symmetric for the reflection  $\phi \rightarrow -\phi$ , since the effective Hamiltonian holds the symmetry. Another phase appearing in the second quadrant is then considered to be a broken one. The present cutoff Hamiltonian  $H_{\Lambda_0}$ , however, is not applicable for the phase, since Fock states with negative  $\mu'^2$  are not physical in the sense that tachyons come out. In general, light-front Hamiltonians

are different between the phases, while their vacua are always equal to the Fock vacuum. This is explicitly shown in two-dimensional  $\phi^4$  model [6,20,21]; for the symmetric phase the Hamiltonian contains oscillatory modes only, while for the broken phase it includes both zero and oscillatory ones. The Hamiltonian for the broken phase has a new mass term produced by the zero mode in addition to the original one  $\mu^2$ , so one can define Fock states with the sum, even if  $\mu^2$  is negative. Further discussion on the broken phase is made in sec. III C.

### C. The RG equations for the broken phase

The RG equation (3.21) is valid for the symmetric phase, but not for the broken one, as shown in subsection III B. The failure stems from the fact that the present  $H_{\Lambda_0}$  does not contain the zero ( $k^+ = 0$ ) mode. The zero mode is responsible for the phase transition, because the order parameter  $\langle 0|\phi|0\rangle$  can not become nonzero without the zero mode, that is, the order parameter is zero for any oscillator ( $k^+ > 0$ ) mode. Hence the present  $H_{\Lambda_0}$  is valid only for the symmetric phase in which  $\langle 0|\phi|0\rangle = 0$ .

There are two ways of finding a Hamiltonian valid for the broken phase. One way is to treat the zero mode explicitly [5,6,20,21]. For this purpose  $\phi^4$  theory is usually quantized in a spatial box  $-L < x^- \leq L$  under the periodic boundary condition, so that the zero mode is separated from the oscillator ( $k^+ > 0$ ) ones. The resulting bare Hamiltonian is different from the present  $H_{\Lambda_0}$  in the sense that the bare Hamiltonian contains not only the oscillator modes but also the zero mode. The zero mode is an operator-valued function of the oscillator modes, since the zero mode satisfies a constraint [5]

$$\int_{-L}^L dx^- \left\{ (\mu^2 - \partial_{\perp}^2) \phi(x) + \frac{\lambda}{3!} \phi^3(x) \right\} = 0. \quad (3.23)$$

This has been obtained by integrating the equation of motion over  $x^-$ . In general, it is not easy to solve the operator-valued nonlinear equation for the zero mode without perturbation in order to treat spontaneous symmetry breaking. A trial is reported for  $\phi^4$  model in two dimensions. In the work [6], the equation is symmetrically ordered and approximately

solved under the Tamm-Dancoff truncation. However, it is not clear how we should order the equation, since the zero mode is not a dynamical operator.

Another way is to add counterterms to the present  $H_{\Lambda_0}$  which has no zero mode [11,18,19]. Only the zero mode can make the order parameter  $\langle 0|\phi|0\rangle$  nonzero. This means that the system has to sit in the bottom of the effective potential, as soon as the zero mode is discarded from  $\phi$ . So we shift  $\phi$  as  $\phi \rightarrow \phi - v$ , and determine a value of  $v$  on a renormalization trajectory. In terms of the shifted field  $\phi$  the Lagrangian density becomes

$$\mathcal{L} = \frac{1}{2}\partial_\mu\phi\partial^\mu\phi - \frac{1}{2}m^2\phi^2 - w\phi - \frac{g}{3!}\phi^3 - \frac{\lambda}{4!}\phi^4, \quad (3.24)$$

where

$$w = v\mu^2 + \frac{\lambda}{3!}v^3, \quad m^2 = \mu^2 + \frac{\lambda v^2}{2}, \quad g = v\lambda, \quad (3.25)$$

where a constant term has been discarded, because it is irrelevant to physics. The light-front Hamiltonian is then

$$H = \int d^3x \left\{ \frac{1}{2} \left[ \sum_{i=1}^2 (\partial_i\phi)^2 + m^2\phi^2 \right] + \frac{g}{3!} : \phi^3 : + \frac{\lambda}{4!} : \phi^4 : \right\}. \quad (3.26)$$

As a feature of the naive light-front field theory which does not treat the zero mode, the linear term in  $\phi$  vanishes. Following the RG procedure shown in the previous subsections, one has RG equations for  $m^2$ ,  $g$  and  $\lambda$ . Inserting (3.25) into the equations yields RG equations for the original parameters  $\mu^2$ ,  $\lambda$  and  $v$ ,

$$\frac{d\lambda}{dt} = \frac{3\zeta}{4\pi} \frac{dI_A}{dt} \lambda^2, \quad \frac{dv}{dt} = 0, \quad \frac{d\mu^2}{dt} = -\frac{\zeta}{8\pi} \frac{dI_A}{dt} (\lambda v)^2. \quad (3.27)$$

The solution to (3.27) is easily obtained as

$$\begin{aligned} \lambda(\Lambda) &= \frac{\lambda_0}{1 - 3\zeta\tilde{A}\lambda_0/(4\pi)}, \\ v(\Lambda) &= v_0, \\ \mu(\Lambda)^2 &= \mu_0^2 + \frac{\lambda_0 v_0^2}{6} \left\{ 1 - \frac{1}{1 - 3\zeta\tilde{A}\lambda_0/(4\pi)} \right\}, \end{aligned} \quad (3.28)$$

where all parameters at  $\Lambda = \Lambda_0$  are characterized by a subscript “0”. For  $\Lambda \gg \Lambda_{phys}$ ,  $A$  tends to  $4\pi t$  in (3.28), indicating no  $M_i$  dependence of the solution in the limit. The

corresponding parameters,  $\mu'$ ,  $\lambda'$  and  $v'$ , present in  $T[H_\Lambda]$  are then obtained by  $\mu'(\Lambda) = \mu(\Lambda)\Lambda_0/\Lambda$ ,  $\lambda'(\Lambda) = \lambda(\Lambda)$  and  $v'(\Lambda) = v(\Lambda)\Lambda_0/\Lambda$ . Obviously, one can find a renormalization trajectory on the positive  $v'^2$  axis in the parameter space  $(\lambda', \mu'^2, v'^2)$ , as shown in Fig. 7. The trajectory does not depend on  $M_i$ , since  $\lambda(\Lambda)'$  and  $\mu(\Lambda)'$  are always zero on the axis. The trajectory has thus no state dependence in the present case.

In (3.27), the sum of  $v^2/6$  times the first equation and the third one becomes  $d(\mu^2 + \lambda v^2/6)/dt = 0$ , indicating that  $C \equiv \mu^2 + \lambda v^2/6$  is RG invariant. Thus,  $v$  is a dependent variable obtained by  $\lambda v^2/6 = -\mu^2 + C$ . This is a natural result of the fact that the original theory includes only  $\mu^2$  and  $\lambda$  as physical parameters. The relation between  $v^2$  and the physical parameters should be unique. In fact,  $C$  is determined as follows. The relation becomes  $\lambda' v'^2/6 = -\mu'^2 + C \exp(2t)$  for parameters  $\lambda'$ ,  $v'^2$  and  $\mu'^2$ , and it forms a group of surfaces, each with different  $C$ , in the parameter space. Only a surface with  $C = 0$  contains the critical line ( the positive  $\lambda'$  axis ) between the broken and symmetric phases. The line is a border of the surface, since  $\mu'^2 = -\lambda' v'^2/6 \leq 0$  for positive  $\lambda'$ . The surface can be regarded as the broken phase, since it can be connected to the symmetric one on the critical line. The effective potential should become minimum on the surface, and it is really confirmed in Sec. III D. The surface is also depicted in Fig. 7. The renormalization trajectory is on the surface, as expected. Perry and Wilson also find the same relation without calculating the effective potential [18]. Their derivation is essentially equal to ours, although  $C$  is set to zero a priori in their derivation.

#### **D. Covariant perturbation theory and effective potential**

The RG equations (3.27) based on the present light-front Hamiltonian formalism are compared with those on the covariant (equal-time) perturbation theory. For this purpose we use a cutoff on the Euclidean momentum,  $\Lambda^2 < k^2$ , and make the same approximations, that is, the one-loop approximation and dropping irrelevant operators. The resultant RG equations are

$$\begin{aligned}\frac{d\lambda}{dt} &= \frac{3\zeta\lambda^2}{(1+r)^2}, & \frac{dg}{dt} &= \frac{3\zeta\lambda g}{(1+r)^2}, & \frac{dm^2}{dt} &= -\frac{\zeta\lambda\Lambda^2}{1+r} + \frac{\zeta g^2}{(1+r)^2}, \\ \frac{dw}{dt} &= -\frac{\zeta g\Lambda^2}{1+r},\end{aligned}\tag{3.29}$$

where  $r = m^2/\Lambda^2$ . Inserting relation (3.25) into (3.29) yields RG equations for the original parameters,

$$\frac{d\lambda}{dt} = \frac{3\zeta\lambda^2}{(1+r)^2}, \quad \frac{dv}{dt} = 0, \quad \frac{d\mu^2}{dt} = -\frac{\zeta\lambda\Lambda^2}{1+r} + \frac{\zeta(\lambda v)^2}{2(1+r)^2}.\tag{3.30}$$

In the derivation of (3.30) from (3.29), the number of equations is reduced from 4 to 3. One of four equations in (3.29) is thus not independent under the condition (3.25). For  $\Lambda$  much larger than  $m$  and  $M_i$ , (3.30) agree with (3.27), except (3.30) newly have a term  $-\zeta\lambda\Lambda^2/(1+r)$  in its third equation. The term comes from the tadpole (Fig.1), but in the present formalism the self mass has already been included in the mass parameter  $\mu$  by taking the normal ordered Hamiltonian. Hence, the RG equations obtained in the light-front Hamiltonian formalism are essentially equal to equations (3.30) calculated in the covariant perturbation theory. Of course, the two RG equations are not identical except the large  $\Lambda$  limit, because regularization schemes are different between the two formulations. The light-front perturbation theory is formally equivalent to the covariant one [16], if the same regularization scheme is taken. In fact, as soon as the  $k^-$  integration is made in the covariant formalism, one finds a direct connection between diagrams obtained in the covariant theory and time-ordered ones in the present formalism.

The equality guarantees that within the framework of the light-front Hamiltonian formalism we can calculate the effective potential through the following ordinary procedure. In the covariant perturbation theory, the effective potential  $V(\phi_{cl})$  is obtained as  $\mu_R^2\phi_{cl}^2/2 + \lambda_R\phi_{cl}^4/4!$  within the present approximations, where  $\mu_R$  and  $\lambda_R$  stand for renormalized quantities and  $\phi_{cl}$  for the classical field, that is, the vacuum expectation value ( $v$ ) of  $\phi$  which is not shifted. The renormalized quantities are solutions  $\mu(\Lambda)$  and  $\lambda(\Lambda)$  at the small  $\Lambda$  limit to RG equations (3.30) under the condition  $v = 0$ , because  $\mu_R$  ( $\lambda_R$ ) are just the sum of one-particle irreducible diagrams produced by an interaction  $\lambda\phi^4$  with 2 (4) external lines. In fact, the

solutions are

$$\begin{aligned}\lambda(\Lambda)\Big|_{\Lambda=0} &= \lambda_0 - \frac{3}{2}\zeta\lambda_0^2 \left\{ \ln \left| \frac{\Lambda_0^2 + \mu_0^2}{\mu_0^2} \right| - \frac{\Lambda_0^2}{\Lambda_0^2 + \mu_0^2} \right\} + O(\hbar^2) \\ \mu(\Lambda)^2\Big|_{\Lambda=0} &= \mu_0^2 - \frac{1}{2}\zeta\lambda_0 \left\{ \Lambda_0^2 - \mu_0^2 \ln \left| \frac{\Lambda_0^2 + \mu_0^2}{\mu_0^2} \right| \right\} + O(\hbar^2)\end{aligned}\quad (3.31)$$

at the one-loop level, and they agree with  $\mu_R$  and  $\lambda_R$  directly calculated with the covariant perturbation theory. Also in the light-front Hamiltonian formalism,  $\mu_R$  and  $\lambda_R$  are obtained from the solutions (3.28) by setting  $\Lambda$  to the small  $\Lambda$  limit ( $2\mu$ ) and  $v$  to zero. The  $\lambda_R$  thus obtained contains not only contributions of the one-loop diagrams (Fig. 2) but also those of the ladder diagrams. All the contributions should be included in  $\lambda_R$ , since they all are one-particle irreducible diagrams. It is then found that  $\mu_R = \mu_0$  and  $\lambda_R = \lambda_0/(1 - a\lambda_0)$  for  $a = 3\zeta\tilde{A}/(4\pi)$  at  $\Lambda = 2\mu$ : Conversely, (i)  $\mu_0 = \mu_R$  and  $\lambda_0 = \lambda_R/(1 + a\lambda_R)$ . The condition  $dV(\phi_{cl})/d\phi_{cl} = 0$  on which the effective potential is minimum leads to (ii)  $6\mu_R^2 = -\lambda_R\phi_{cl}^2$ . RG equations (3.27) are now solved under the initial conditions (i) and (ii); of course  $\phi_{cl}$  is identified with  $v$ . As mentioned in sec. III C,  $C \equiv \mu(\Lambda)^2 + \lambda(\Lambda)v(\Lambda)^2/6$  is RG invariant. For any  $\Lambda$  it becomes  $-av_0^2\lambda_R^2/(1 + a\lambda_R)$ , because of relations (i) and (ii). In the large  $\Lambda_0$  limit, the quantity  $a$  diverges, so that  $C$  tends to  $-v_0^2\lambda_R$  for  $\lambda_R = \lambda_0/(1 - a\lambda_0) \rightarrow 0$ . Hence,  $C$  is zero in the limit, as far as  $v_0$  is finite. This is a reflection of the fact that  $\lambda_R$  is forced to vanish in the limit, that is, the present model is trivial. The condition for the system to be in the bottom of the effective potential is then  $\mu(\Lambda)^2 + \lambda(\Lambda)v(\Lambda)^2/6 = 0$ . It agrees with the result shown in subsection III C.

### ACKNOWLEDGMENTS

We would like to acknowledge stimulating discussions with our colleagues in Kyushu University, in particular S. Tominaga. Support of this work is provided by a Grant-in-Aid for Scientific Research from the Ministry of Education, Science and Culture of Japan (No. 06640404).

## APPENDIX A: LOOP INTEGRALS

The loop integral  $A$  is easily performed by introducing the Jacobi coordinate  $(x, \mathbf{r})$  defined with  $\mathbf{k}_1 = (xP^+, x\mathbf{P}_\perp + \mathbf{r})$ ,  $\mathbf{k}_2 = ((1-x)P^+, (1-x)\mathbf{P}_\perp - \mathbf{r})$ . The result is  $A = I_A(\Lambda_{n-1}) - I_A(\Lambda_n)$  with

$$\begin{aligned}
 I_A(\Lambda) &\equiv 2 \int dx d\mathbf{r} \frac{\theta(x(1-x)\Lambda^2 - \mathbf{r}^2 - \mu^2)}{x(1-x)M^2 - \mathbf{r}^2 - \mu^2} \\
 &= 2\pi \ln \left| \frac{1 - \sqrt{a(\Lambda)}}{1 + \sqrt{a(\Lambda)}} \right| - 2\pi \sqrt{a(M)} \ln \left| \frac{\sqrt{a(\Lambda)} - \sqrt{a(M)}}{\sqrt{a(\Lambda)} + \sqrt{a(M)}} \right| \theta(a(M)) \\
 &\quad + 4\pi \sqrt{-a(M)} \arctan \left\{ \frac{\sqrt{a(\Lambda)}}{\sqrt{a(-M)}} \right\} \theta(-a(M))
 \end{aligned} \tag{A1}$$

for  $\Lambda \geq 2\mu$  and zero for  $\Lambda < 2\mu$ , where  $a(z) = 1 - 4\mu^2/z^2$ .

The loop integral  $B$  is also given in a similar fashion. As an example let us consider the diagram of Fig. 3, in which particles 1 and 2 interact with each other, while particle 3 is free. Each has a momentum  $\mathbf{k}_i$  in the initial state and  $\mathbf{k}'_i$  in the intermediate state. For convenience we introduce the Jacobi coordinates

$$\begin{aligned}
 \mathbf{k}_1 &= (x(1-y)P^+, x[(1-y)\mathbf{P}_\perp - \mathbf{s}] + \mathbf{r}), \\
 \mathbf{k}_2 &= ((1-x)(1-y)P^+, (1-x)[(1-y)\mathbf{P}_\perp - \mathbf{s}] - \mathbf{r}), \\
 \mathbf{k}_3 &= (yP^+, y\mathbf{P}_\perp + \mathbf{s}).
 \end{aligned} \tag{A2}$$

The momentum  $(x, \mathbf{r})$  represents a relative motion between interacting two particles in the initial state, and  $(x', \mathbf{r}')$  the motion in the intermediate state. On the other hand,  $(y, \mathbf{s})$  is a conserved momentum describing a relative motion between the interacting pair and the third particle. The quantity  $B$  is obtained by making integrations over  $x'$  and  $\mathbf{r}'$ , so it is eventually given as a function of  $y$  and  $\mathbf{s}$ :  $B \equiv I_B(\Lambda_{n-1}) - I_B(\Lambda_n)$  with

$$\begin{aligned}
 I_B(\Lambda) &= 2\pi \ln \left| \frac{1 - \sqrt{b(\Lambda)}}{1 + \sqrt{b(\Lambda)}} \right| - 2\pi \sqrt{b(M)} \ln \left| \frac{\sqrt{b(\Lambda)} - \sqrt{b(M)}}{\sqrt{b(\Lambda)} + \sqrt{b(M)}} \right| \theta(b(M)) \\
 &\quad + 4\pi \sqrt{-b(M)} \arctan \left\{ \frac{\sqrt{b(\Lambda)}}{\sqrt{-b(M)}} \right\} \theta(-b(M))
 \end{aligned} \tag{A3}$$

for  $\Lambda \geq \mathcal{M}$  and zero for  $\Lambda < \mathcal{M}$ , where  $s^2 \equiv s_1^2 + s_2^2$  and

$$b(z) \equiv \frac{(z^2 - \mathcal{M}^2)(1 - y)}{(z^2 - \mathcal{M}^2)(1 - y) + (2\mu)^2}, \quad \mathcal{M}^2 \equiv \frac{(2\mu)^2}{1 - y} + \frac{\mu^2}{y} + \frac{s^2}{y(1 - y)} \geq (3\mu)^2. \quad (\text{A4})$$

The invariant mass  $M$  of the initial state is smaller than  $\Lambda_{n-1}$ , since the state is in the  $\mathcal{P}$  space. The mass is related to  $\mathcal{M}$  as

$$M^2 \equiv \frac{\mu^2 + r^2}{(1 - y)x(1 - x)} + \frac{\mu^2}{y} + \frac{s^2}{y(1 - y)} \geq \mathcal{M}^2 \geq (3\mu)^2, \quad (\text{A5})$$

where use has been made of the inequality  $(\mu^2 + r^2)/(x(1 - x)) \geq (2\mu)^2$ . Equation (A5) indicates that  $\mathcal{M}$  is somewhere between  $3\mu$  and  $M$ . The  $\mathcal{M}$  is conserved during the process Fig. 3, since it is a function of the conserved momentum ( $y, s$ ). In Fig. 4,  $B$  is drawn as a function of  $\mathcal{M}^2$  and  $y$  (instead of  $s^2$  and  $y$ ) and compared with  $A$ . For  $\Lambda_{n-1} = 100\Lambda_{phys}$ , in Fig. 4(a),  $B$  agrees with  $A$  at all  $\mathcal{M}$  and  $y$ . The agreement becomes poor gradually as  $\Lambda$  decreases to  $2\mu$ . For example, for  $\Lambda_{n-1} = 10\Lambda_{phys}$  in Fig. 4(b),  $B$  is close to  $A$  at  $\mathcal{M} < 0.8\Lambda_{n-1}$ , but undershoots  $A$  for  $0.9\Lambda_{n-1} < \mathcal{M} < \Lambda_{n-1}$ , indicating that  $B$  can be approximated into  $A$  for any initial state with  $M$  less than  $0.8\Lambda_{n-1}$ .

## REFERENCES

- [1] R. J. Perry, A. Harindranath and K. G. Wilson, Phys. Rev. Lett **65**, 2959(1990).
- [2] I. Tamm, J. Phys. (USSR)**9**, 449(1945); S. M. Dancoff, Phys. Rev. **78**, 382(1950); H. A. Bethe and F. D. Hoffman, *Mesons and Fields*(Row, Peterson, Evanson, 1955)Vol. II; E. M. Henley and W. Thirring, *Elementary Quantum Field Theory*(McGraw-Hill, New York, 1962)
- [3] K. Harada, T. Sugihara, M. Taniguchi and M. Yahiro, Phys. Rev. **D49**, 4226(1994).
- [4] T. Sugihara, M. Matsuzaki and M. Yahiro, Phys. Rev. **D**, to be published.
- [5] T. Maskawa and K. Yamawaki, Prog. Theor. Phys. **56**, 270(1976);
- [6] S. S. Pinsky and B. van de Sande, Phys. Rev. **D49**, 2001(1994).
- [7] D. Mustaki, S. S. Pinsky, J. Shigemitsu and K. G. Wilson, Phys. Rev. **D43**, 3411(1991)
- [8] O. Abe, K. Tanaka and K. G. Wilson, Phys. Rev. **D48**, 4856(1993)
- [9] St. Głazek, A. Harindranath, S. S. Pinsky, J. Shigemitsu and K. G. Wilson, Phys. Rev. **D47**, 1599(1993).
- [10] K. G. Wilson and J. Kogut Phys. Rep. **C12**, 75(1974).
- [11] R. J. Perry Ann. Phys. (N.Y.)**232**, 116(1994)
- [12] K. G. Wilson and J. Kogut Phys. Rev. **D8**, 1438(1970).
- [13] St. Głazek and K.G. Wilson, Phys. Rev. **D48**, 5863(1993); Phys. Rev. **D49**, 4214(1993).
- [14] C. Bloch, Nucl. Phys. **6**, 328(1958).
- [15] C. Bloch and J. Horowitz, Nucl. Phys. **8**, 91(1958).
- [16] S. -J. Chang, R. G. Root and T. -M. Yan, Phys. Rev. **D7**, 1133(1973). S. -J. Chang and T. -M. Yan, Phys. Rev. **D7**, 1147(1973). T. -M. Yan, Phys. Rev. **D7**, 1760(1973);

- Phys. Rev. **D7**, 1781(1973).
- [17] N. Nakanishi and K. Yamawaki, Nucl. Phys. **B122**, 15(1977).
- [18] P. J. Perry and K.G. Wilson, Nucl. Phys. **B403**, 587(1993)
- [19] K. G. Wilson, T. S. Walhout, A. Harindranath, W. M. Zhang, R. J. Perry and S.t  
Głazek, Phys. Rev. **D49**, 6720(1994).
- [20] C. M. Bender, S. S. Pinsky and B. van de Sande, Phys. Rev. **D48**, 816(1993).
- [21] S. S. Pinsky, B. van de Sande and J. R. Hiller Phys. Rev. **D51**, 726(1995).

## FIGURES

FIG. 1. Tadpole(one-loop self-mass) diagram. The divergent contribution of the diagram is renormalized by a redefinition of the mass parameter  $\mu^2$ .

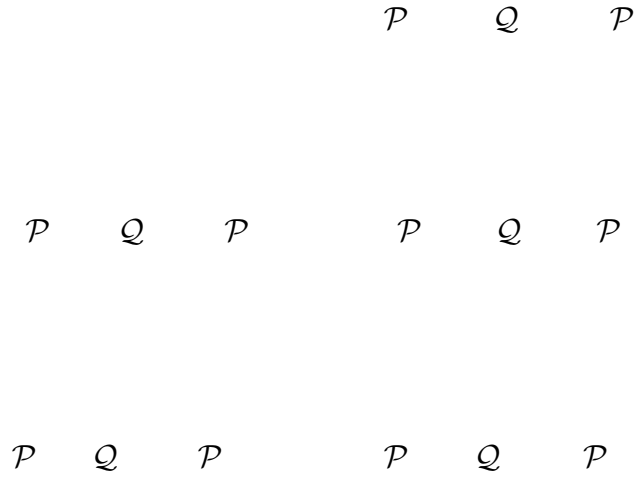


FIG. 2. One-loop diagrams which contribute to the matrix elements of  $\mathcal{P}(V + VQG_0QV)\mathcal{P}$  between two-body states.



FIG. 3. An example of the one-loop diagrams which contribute to the matrix elements of  $\mathcal{P}(V + VQG_0QV)\mathcal{P}$  between three-body states.

$\mathcal{M}/\Lambda_{n-1}$  $\mathcal{M}/\Lambda_{n-1}$ 

FIG. 4. The loop integrals  $A$  and  $B$  as a function of  $\mathcal{M}$  and  $y$ ; these are defined in Appendix A. The integral  $A$  is plotted by the solid line, and  $B$  by dots. Each curve, which is given by connecting the dots, has different  $y$ , from 0.1 to 0.9 with an interval 0.1:  $B$  decreases as  $y$  goes down with  $\mathcal{M}$  fixed. Different parameter sets are taken in (a) and (b): (a)  $\Lambda_{\text{phys}} = M_i = \mu = 0.01\Lambda_{n-1}$ . (b)  $\Lambda_{\text{phys}} = M_i = \mu = 0.1\Lambda_{n-1}$ .

$$\mathcal{P} \quad \mathcal{Q} \quad \mathcal{P}$$

FIG. 5. A unique one-loop diagram which contributes to the matrix elements  $\mathcal{P}(V + V\mathcal{Q}G_0\mathcal{Q}V)\mathcal{P}$  between one- and three-body states.

$\lambda'$

$\mu'^2/\Lambda_0^2$

FIG. 6. A flow diagram for the lowest eigenstate with  $M_1/\Lambda_0 = 0.01$ . The vertical and horizontal axes mean  $\mu'^2$  and  $\lambda'$ , respectively. The first quadrant ( $\lambda' > 0$ ,  $\mu'^2 > 0$ ) corresponds to the symmetric phase. The renormalization trajectory exists on the positive  $\mu'^2$  axis and the critical line on the positive  $\lambda'$  axis. Flows are plotted with initial conditions,  $\mu'_0/\Lambda_0 = 0.2, 0.6, 1.0, 1.4, 1.8$  and  $\lambda'_0 = 1.0$ , and with a step  $\delta\Lambda/\Lambda_0 = 0.001$ .

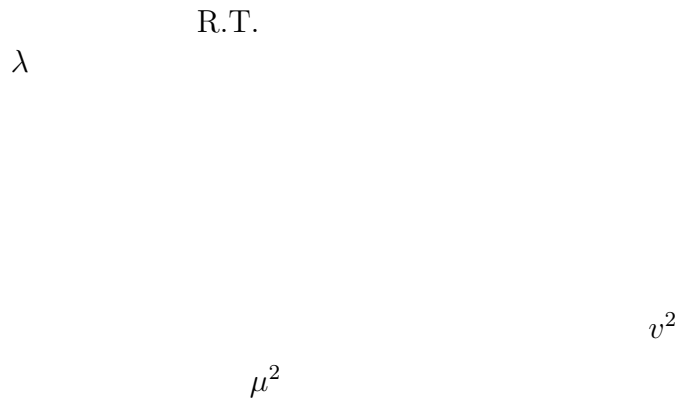
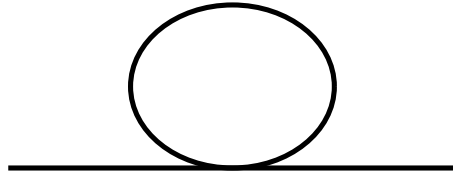
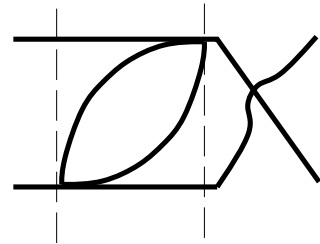
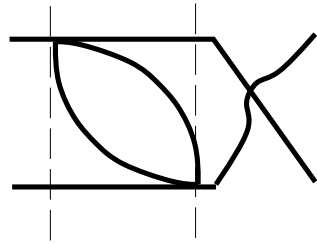
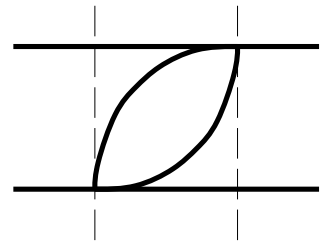
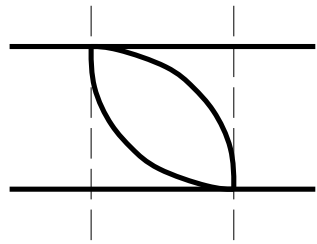
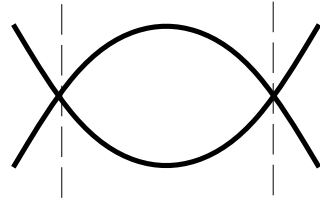
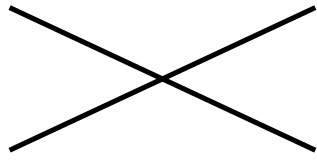
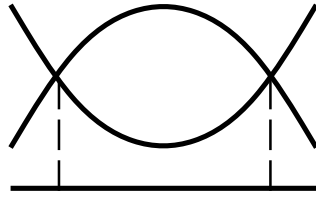
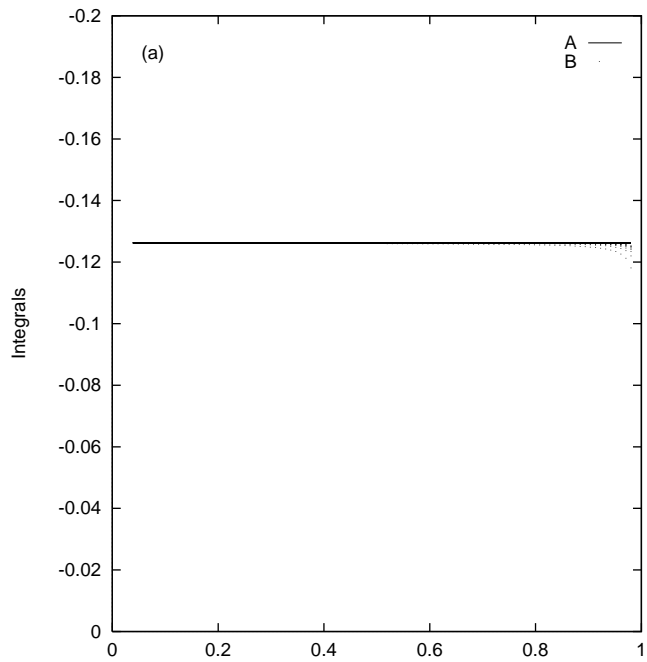


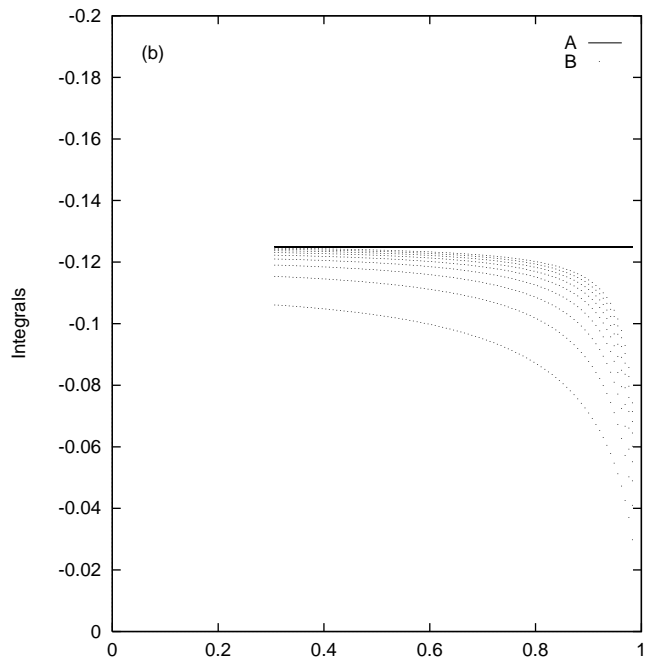
FIG. 7. A flow diagram for the lowest eigenstate is on the surface  $\mu^2 + v^2\lambda/6 = 0$  corresponding to the broken phase. The renormalization trajectory(R.T.) is on the positive  $v^2$  axis.

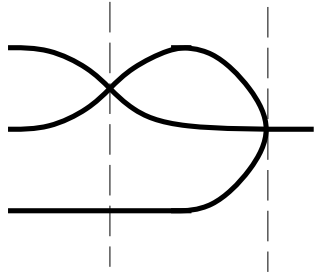


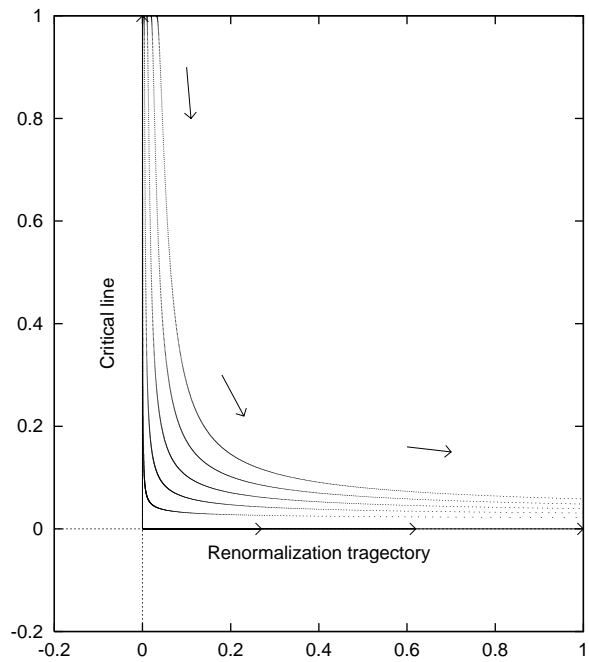












Surface —

